ACTA ABP BIOCHIMICA POLONICA

Vol. 67, No 1/2020
49–52
https://doi.org/10.18388/abp.2020_2896

Regular paper

A crystallization and preliminary X-ray diffraction study of the *Arabidopsis thaliana* proliferating cell nuclear antigen (PCNA2) alone and in a complex with a PIP-box peptide from Flap endonuclease 1*

Ewa Kowalska[1], Wojciech Strzalka[1]✉ and Takuji Oyama[2]✉

[1]Department of Plant Biotechnology, Faculty of Biochemistry, Biophysics and Biotechnology, Jagiellonian University, Kraków, Poland; [2]Faculty of Life and Environmental Sciences, University of Yamanashi, 4-4-37 Takeda, Kofu, Yamanashi 400-8510, Japan

DNA replication is an important event for all living organisms and the mechanism is essentially conserved from archaea, bacteria to eukaryotes. Proliferating cell nuclear antigen (PCNA) acts as the universal platform for many DNA transacting proteins. Flap endonuclease 1 (FEN1) is one such enzyme whose activity is largely affected by the interaction with PCNA. To elucidate the key interactions between plant PCNA and FEN1 and possible structural change of PCNA caused by binding of FEN1 at the atomic level, crystallization and preliminary studies of X-ray diffraction of crystals of *Arabidopsis thaliana* PCNA2 (*At*PCNA2) alone and in a complex with a peptide derived from *At*FEN1, which contains a typical PCNA-interacting protein (PIP)-box motif, were performed. Both peptide-free and peptide-bound *At*PCNA2s were crystallized using the same reservoir solution but in different crystal systems, indicating that the peptide affected the intermolecular interactions in the crystals. Crystals of *At*PCNA2 belonged to the hexagonal space group $P6_3$, while those of the peptide-bound *At*PCNA2 belonged to the rhombohedral space group *H3*, both of which could contain the functional homo-trimers.

Key words: Plant DNA replication, PCNA, FEN1, PIP-box

Received: 24 October, 2019; revised: 03 February, 2020; accepted: 11 February, 2020; available on-line: 19 March, 2020

✉e-mail: wojciech.strzalka@uj.edu.pl (WS); takujio@yamanashi.ac.jp (TO)

***Acknowledgements of financial support**: This project was supported by the National Science Center Poland (project no. Sonata-Bis3/UMO-2013/10/E/NZ1/00749 to WS). This work was partly supported by JSPS KAKENHI Grant Number 18K06081, and also by the Collaborative Research Program of the Institute for Protein Research, Osaka University, CR-18-02 (to TO).

Abbreviations: FEN1, Flap endonuclease 1; PCNA, Proliferating cell nuclear antigen; PIP-box, PCNA-interacting protein (PIP)-box

INTRODUCTION

Genomic DNA replication requires over 50 kinds of protein which work in a highly coordinated manner by forming a large assembly called a replisome (Masai *et al.*, 2010). The mechanism of DNA replication is conserved from archaea, bacteria to eukaryotes. PCNA is one of the most essential proteins involved in DNA metabolic processes such as replication, repair and recombination. PCNA recruits and regulates the DNA metabolizing proteins by tethering them onto DNA (Moldovan *et al.*, 2007). PCNA possesses a ring structure formed by the three identical subunits suitable for encircling DNA. PCNA is topologically linked to DNA by the ATP-dependent action of clamp-loader called RFC (replication factor C) (Yao & O'Donnell, 2012). PCNA binds different proteins involved in DNA metabolism by recognizing the canonical motif called the PCNA-interacting protein (PIP)-box, which is usually located at the C-terminus of the partner protein (Warbrick, 1998). Although the conservation of the PIP-box motif sequence is moderate, the binding mode of PIP-box peptides to PCNA is similar, as shown by many crystallographic studies (Gulbis *et al.*, 1996; Matsumiya *et al.*, 2002; Bubeck *et al.*, 2011). Recently, other PCNA-binding motifs have been identified and characterized by structural biology, which showed the unique binding mode of these non-canonical motifs to PCNAs (Hishiki *et al.*, 2009; Sebesta *et al.*, 2017).

Previously, we studied the functional and structural aspects of *Arabidopsis thaliana* PCNA proteins. They are designated as *At*PCNA1 (molecular mass M_r: 30 508 Da) and *At*PCNA2 (M_r: 30 335 Da), which are in 96% identical to each other, and show significant homology to human and archaeal PCNAs (Strzalka *et al.*, 2009). We determined the atomic structure of the two Arabidopsis PCNAs complexed with the canonical PIP-box peptide derived from human cyclin-dependent kinase inhibitor, p21/WAF-1, using X-ray crystallography. The structure of the plant PCNAs showed the basic conservation in comparison to human and archaeal PCNA, and a possible functional binding mode of the PIP-box. Flap endonuclease 1 (FEN1) is a structure-specific nuclease which removes the 5' protruded flap nucleotide generated during DNA replication and repair. In particular, the removal of RNA primers from the nascent strands in DNA replication by the action of FEN1 is essential for the maturation of Okazaki fragments. Human FEN1 activity is stimulated by the interaction with PCNA via the PIP-box peptide (Chapados *et al.*, 2004; Bruning & Shamoo, 2004). The crystal structures of human and archaeal FEN1s in various states such as FEN1 alone (Hwang *et al.*, 1998; Hosfield *et al.*, 1998), in complexes with DNA (Chapados *et al.*, 2004; Tsutakawa *et al.*, 2011) or with PCNA (Sakurai *et al.*, 2005; Doré *et al.*, 2006) were investigated. However, corresponding studies related to the plant FEN1 were not reported yet.

To explore the structural aspects of plant PCNA and FEN1 interactions, including possible structural change of PCNA associated with binding of FEN1, crystallographic studies of the Arabidopsis PCNA2-FEN1 PIP-box peptide complex as well as the isolated form of *At*PCNA2 were performed. Here, we describe the purification, crystallization and study of the preliminary X-ray diffraction of *At*PCNA2 alone and its complex with a PIP-box peptide derived from the Arabidopsis FEN1. In particular, we for the first time succeeded in the crystallization of the peptide-free *At*PC-

Table 1. Data collection and processing

Protein complex	*At*PCNA2	*At*PCNA2-Fen1 PIP complex
Diffraction source	Rigaku MicroMax-007 HF	Rigaku FR-E
Wavelength (Å)	1.5418	1.5418
Temperature (K)	100	100
Detector	R-AXIS VII	R-AXIS VII
Crystal-to-detector distance (mm)	200	175
Rotation range per image (°)	0.5	0.5
Exposure time per image (s)	300	270
Space group	$P6_3$	*H*3
Unit cell constants		
a, *b*, *c* (Å)	93.95, 93.95, 63.54	224.17, 224.17, 199.73
α, *β*, *γ* (°)	90, 90, 120	90, 90, 120
Mosaicity (°)	0.30	0.10
Resolution range (Å)	50.0-2.65 (2.78-2.65)	50.0-2.85 (2.90-2.85)
Total No. of observed reflections	63 486 (8383)	366 082 (18 559)
No. of unique reflections	9385 (1228)	87 329 (4497)
Completeness (%)	99.8 (99.5)	99.9 (100.0)
Multiplicity	6.8 (6.8)	4.2 (4.1)
$I/\sigma(I)$	22.2 (3.1)	9.5 (2.2)
R_{meas}	0.068 (0.735)	0.185 (0.863)
R_{merge}	0.057 (0.623)	0.142 (0.658)
Half-set correlation $CC_{1/2}$	0.999 (0.791)	0.990 (0.654)
Overall B factor from Wilson plot (Å^2)	57.6	31.9

Values for the outer shell are given in parentheses.

NA2, which allows revealing the possible structural change of *At*PCNA2 caused by the binding of DNA metabolizing proteins such as *At*FEN1.

MATERIALS AND METHODS

Overexpression and Purification. The *Escherichia coli* BL21 (DE3) Rosetta strain (Novagen) was used for *At*PCNA2 protein production. Cells transformed with pET15b vector coding for *At*PCNA2 (Strzalka *et al.*, 2009) fused with histidine tag were grown at 310 K using LB medium supplemented with 30 mg l^{-1} chloramphenicol and 100 mg l^{-1} ampicillin. Protein overexpression was induced using 1 mM isopropyl β-D-1-thiogalactopyranoside (IPTG) when OD_{600} of the culture reached ~0.5. Bacteria were cultured by shaking vigorously at 310 K for 4 h then followed by centrifugation (10 min, 12000×*g*, 277 K). The pellet from 1 l of culture was resuspended in 40 ml of binding buffer A (50 mM sodium phosphate, 300 mM NaCl, 20 mM imidazole, pH 7.5) which contained an EDTA-free protease inhibitor cocktail (Roche). Bacteria were sonicated for 15 min (5 s pulse followed by a 15 s pause, QSonica Q700 sonicator, USA). The cell lysate containing the *At*PCNA2 protein was supplemented with 200 units of DNase I (Takara Bio, Japan) and incubated for 20 min on ice. Then, the lysate was centrifuged (20 min, 21000×*g*, 277 K) and the supernatant was loaded onto HisTrap FF Ni Sepharose (5 ml, GE Healthcare, Sweden). The protein was purified according to the protocols supplied by the manufacturers. After being eluted from the nickel resin, the *At*PCNA2 was dialyzed into buffer B (50 mM Tris–HCl pH 7.6) and loaded onto the anion exchange HiTrap Q column (5 ml, GE Healthcare, Sweden). The protein elution was performed using a linear NaCl gradient from 0 to 1 M (10 volumes of the column). The protein was eluted when NaCl concentration was around 0.5 M NaCl. The purified *At*PCNA2 was dialyzed against buffer C (50 mM Tris–HCl, 200 mM NaCl, 0.2 mM EDTA, pH 8.0), supplemented with glycerol (final

concentration 15% (*v*/*v*)) and stored at 193 K for further experiments.

The 22-amino acid long peptide containing the PCNA interacting protein (PIP)-box from *A. thaliana* endonuclease FEN1 (334-KNKSSQGRLESFFKPVANSSVP-355) was commercially synthesized (LifeTein LLC, New Jersey, USA).

Crystallization. The protein was crystallized using the hanging-drop vapour diffusion method at 293 K. According to the previous crystallization experiment of *At*PCNAs complexed with human p21 peptide (Strzalka *et al.*, 2009), a reservoir containing 100 mM citric acid pH 4.5 and 1.2 to 1.8 M ammonium sulfate was used for both *At*PCNA2 alone and the complex with the peptide. *At*PCNA2 used for crystallization was concentrated to 20 mg ml^{-1} in buffer C deprived of glycerol. In the case of the complex crystallization, the peptide was added to the protein at a 1.5 molar ratio (assuming *At*PCNA2 as a monomer) and incubated at 289 K for 30 min. Crystallization drops were produced by mixing equal volumes (1 µl) of the protein and reservoir solutions and then placed against the reservoir solution (500 µl). Crystals of the peptide-free and peptide-bound *At*PCNA2s grew to a maximum dimension of approximately 200 µm within a week.

X-ray diffraction data collection. X-ray diffraction data were collected using an in-house imaging plate detector R-AXIS VII (Rigaku) equipped with an X-ray generator either MicroMax-007 HF or FR-E (Rigaku). Crystals were cryo-harvested by soaking them into the mother liquor supplemented with either 30% (*v*/*v*) ethylene glycol for *At*PCNA2 crystals or 20% (*v*/*v*) glycerol for the *At*PCNA2-*At*FEN1 PIP-box peptide complex for several seconds, and then flash-cooled in liquid nitrogen. The detailed X-ray diffraction experiment conditions and the data statistics are listed in Table 1. The data were processed by the XDS (Kabsch, 2010), Pointless (Evans, 2006), and Aimless (Evans & Murshudov, 2013) programs. The number of molecules in the asymmetric units was estimated using the Matthews coefficients (Matthews, 1968).

RESULTS AND DISCUSSION

Crystallization

We previously succeeded in crystallizing the human p21-derived peptide-bound plant PCNAs which were purified using HisTrap as the only column chromatography method (Strzalka *et al.*, 2009). In this study, using two-step column chromatography we purified *At*PCNA2 (Fig. 1). The genomic DNA from the *E. coli* cells was degraded into small fragments during sonication and DNase I treatment. Next, most of these fragments were removed at the first stage of the protein purification when the HisTrap column was used. The DNA remaining in the protein sample eluted from the HisTrap column was separated from *At*PCNA2 using the HiTrap Q column (data not shown). Using a protein sample of higher purity than previously (Strzalka *et al.*, 2009) we were able to crystallize *At*PCNA2 free of the ligand as well as complexed with the PIP-box peptide derived from the *At*FEN1. Interestingly, both the peptide-free and peptide-bound *At*PCNA2 crystallized under the same reservoir conditions but in different crystal forms (Fig. 2), as revealed by the following crystallographic analysis. The peptide used for the present study affected the packing interactions of *At*PCNA2 in the crystals.

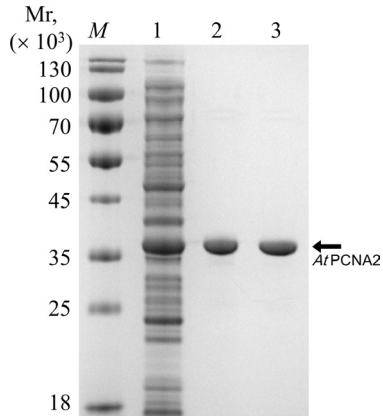

Figure 1. Purification of *At*PCNA2. (*a*) SDS-PAGE analysis (12%) of *At*PCNA2 after each purification step. The proteins were stained using Coomassie Brilliant Blue.
Lanes: M, molecular mass standards with sizes indicated on the left; 1, *E. coli* supernatant after sonication containing *At*PCNA2; 2, *At*PCNA2 after purification using HisTrap Ni-chelating affinity chromatography; 3, *At*PCNA2 purified using HisTrap Ni-chelating affinity chromatography followed by HiTrap Q anion-exchange chromatography.

X-ray crystallographic study

The *At*PCNA2 crystals diffracted the X-rays from an in-house generator to a resolution of 2.65 Å, and the *At*PCNA2-*At*FEN1 PIP-box peptide complex to 2.85 Å (Fig. 3 and Table 1). The *At*PCNA2 crystals alone belong to the hexagonal space group $P6_3$, with unit cell constants of $a=b=93.95$ Å, $c=63.54$ Å, and probably contain the one subunit in the asymmetric unit with a Matthews coefficient (V_M) of 2.68 $Å^3$ Da^{-1} and a solvent content of 54%. These crystallographic parameters are similar to those for homologous PCNAs (Matsumiya *et al.*, 2001; Ladner *et al.*, 2011) which suggests that in the *At*PCNA2 crystals monomers form homotrimers with crystallographic symmetry-related molecules. On the other hand, the *At*PCNA2-*At*FEN1 PIP-box peptide complex crystals belong to the space group *H*3 with unit cell constants of $a=b=224.17$ Å, $c=199.73$ Å. The space group and unit cell constants of the crystal of this complex are similar to those of the previous *At*PCNA2-human p21 peptide complex crystal which contains eight complex molecules in the asymmetric unit with two monomers that form the symmetry-related homotrimers and the two independent homotrimers. If the crystal of the *At*PCNA2/*At*FEN1 PIP-box peptide complex has a molecular arrangement in the crystal very similar to that

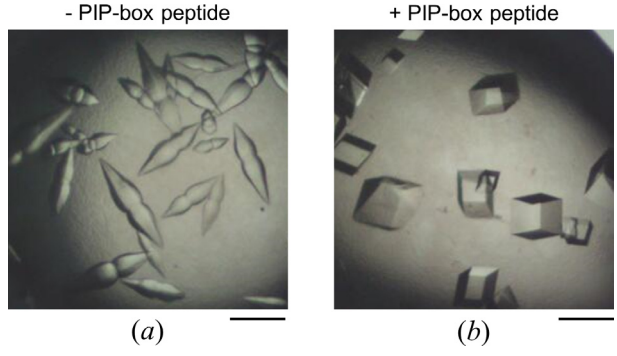

Figure 2. Crystals of (*a*) ligand-free *At*PCNA2 and (*b*) *At*PCNA2-FEN1 PIP-box peptide complex.
The scale bar is 100 µm.

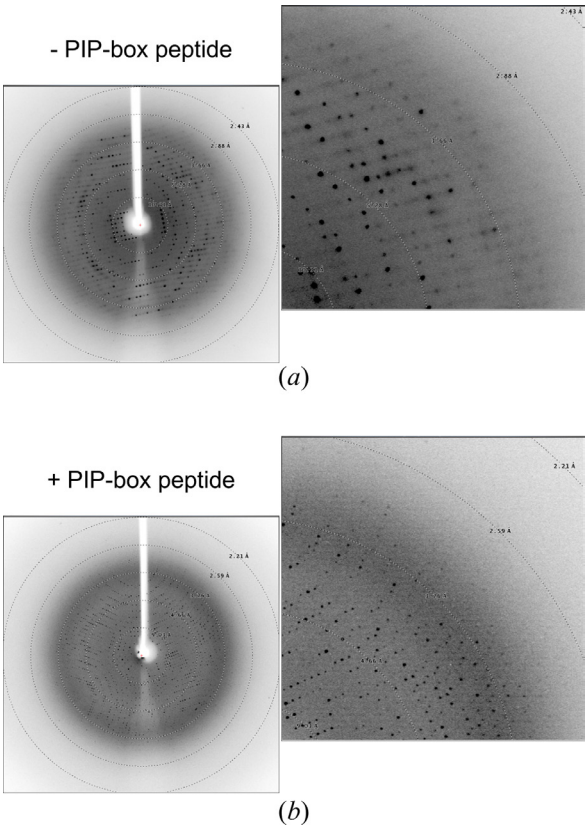

Figure 3. Diffraction patterns of (*a*) ligand-free *At*PCNA2 and (*b*) *At*PCNA2-FEN1 PIP-box peptide complex crystals obtained on in-house RIGAKU R-AXIS VII diffractometers.
Enlarged images are also shown next to the full images.

of the *At*PCNA2-human p21 peptide complex, it leads to a V_M of 3.66 Å^{3}Da^{-1} and a solvent content of 66%. Despite the fact that both the peptide-free and peptide-bound *At*PCNA2 proteins were crystallized using the same reservoir solution, two different forms of crystals were obtained, one type for *At*PCNA2 and the other for peptide-bound *At*PCNA2. Determining the structure of these complexes at the atomic level would give us an answer whether the peptide-bound *At*PCNA2 complex displays unique and different inter-homotrimer interactions in the crystal, as compared to those in the ligand-free *At*PCNA2 crystal. This information would be significant in the context of a detailed understanding of the role of PCNA in FEN1-dependent DNA replication in plants. Although we solved both crystal structures by the molecular replacement method, the quality of the electron density maps was too poor to build accurate atomic models. Therefore, the preparation of the better quality crystals is in progress to obtain high-quality X-ray diffraction data at synchrotron radiation facility beamlines.

Acknowledgement

The Faculty of Biochemistry, Biophysics and Biotechnology is a partner of the Leading National Research Center (KNOW) supported by the Ministry of Science and Higher Education. We thank Drs. Tsuyoshi Inoue and Yohta Fukuda for giving us an opportunity to use the X-ray diffractometer in their laboratory, and Drs. Genji Kurisu, Hideaki Tanaka and Tetsuko Nakaniwa for their kind support and encouragement during this research.

REFERENCES

Bubeck D, Reijns MA, Graham SC, Astell KR, Jones EY, Jackson AP (2011) PCNA directs type 2 RNase H activity on DNA replication and repair substrates. *Nucleic Acids Res* **39**: 3652–3666. https://doi.org/10.1093/nar/gkq980

Bruning JB, Shamoo Y (2004) Structural and thermodynamic analysis of human PCNA with peptides derived from DNA polymerase-delta p66 subunit and flap endonuclease-1. *Structure* **12**: 2209–2219. https://doi.org/10.1016/j.str.2004.09.018

Chapados BR, Hosfield DJ, Han S, Qiu J, Yelent B, Shen B,Tainer JA (2004) Structural basis for FEN-1 substrate specificity and PCNA-mediated activation in DNA replication and repair. *Cell* **116**: 39–50. https://doi.org/10.1016/s0092-8674(03)01036-5

Doré AS, Kilkenny ML, Jones SA, Oliver AW, Roe SM, Bell SD, Pearl LH (2006) Structure of an archaeal PCNA1-PCNA2-FEN1 complex: elucidating PCNA subunit and client enzyme specificity. *Nucleic Acid Res* **2006**: 4515–4526. https://doi.org/10.1093/nar/gkl623

Evans PR (2006) Scaling and assessment of data quality. *Acta Cryst* **D62**: 72–82. https://doi.org/10.1107/S0907444905036693

Evans PR, Murshudov GN (2013) How good are my data and what is the resolution? *Acta Cryst* **D69**: 1204–1214. https://doi.org/10.1107/S0907444913000061

Gulbis JM, Kelman Z, Hurwitz J, O'Donnell M, Kuriyan J (1996). Structure of the C-terminal region of p21(WAF1/CIP1) complexed with human PCNA. *Cell* **87**: 297–806. https://doi.org/10.1016/s0092-8674(00)81347-1

Hwang KY, Baek K, Kim HY, Cho Y (1998) The crystal structure of flap endonuclease-1 from *Methanococcusjannaschii*. *Nat Struct Biol* **5**: 707–713. https://doi.org/10.1038/1406

Hishiki A, Hashimoto H, Hanafusa T, Kamei K, Ohashi E, Shimizu T, Ohmori H, Sato M (2009) Structural basis for novel interactions between human translesion synthesis polymerases and proliferating cell nuclear antigen. *J Biol Chem* **284**: 10552–10560. https://doi.org/10.1074/jbc.M809745200

Hosfield DJ, Mol CD, Shen B, Tainer JA (1998). Structure of the DNA repair and replication endonuclease and exonuclease FEN-1: coupling DNA and PCNA binding to FEN-1 activity. *Cell* **95**: 135–146. https://doi.org/10.1016/s0092-8674(00)81789-4

Kabsch W (2010) XDS. *Acta Cryst* **D66**: 125–132. https://doi.org/10.1107/S0907444909047337

Ladner JE, Pan M, Hurwitz J, Kelman Z (2011) Crystal structures of two active proliferating cell nuclear antigens (PCNAs) encoded by *Thermococcus kodakaraensis*. *Proc Natl Acad Sci U S A* **108**: 2711–2716. https://doi.org/10.1073/pnas.1019179108

Masai H, Matsumoto S, You Z, Yoshizawa-Sugata N, Oda M (2010) Eukaryotic chromosome DNA replication: where, when, and how? *Annu Rev Biochem* **79**: 89–130. https://doi.org/10.1146/annurev.biochem.052308.103205

Matsumiya S, Ishino Y, Morikawa K (2001) Crystal structure of an archaeal DNA sliding clamp: proliferating cell nuclear antigen from *Pyrococcus furiosus*. *Protein Sci* **10**: 17–23. https://doi.org/10.1110/ps.36401

Matsumiya S, Ishino S, Ishino Y, Morikawa K (2002) Physical interaction between proliferating cell nuclear antigen and replication factor C from *Pyrococcus furiosus*. *Genes Cells* **7**: 911–922. https://doi.org/10.1046/j.1365-2443.2002.00572.x

Matthews BW (1968) Solvent content of protein crystals. *J Mol Biol* **33:** 491–497. https://doi.org/10.1016/0022-2836(68)90205-2

Moldovan GL, Pfander B, Jentsch S (2007) PCNA, the maestro of the replication fork. *Cell* **129**: 665–679. https://doi.org/10.1016/j.cell.2007.05.003

Sakurai S, Kitano K, Yamaguchi H, Hamada K, Okada K, Fukuda K, Uchida M, Ohtsuka E, Morioka H, Hakoshima T (2005) Structural basis for recruitment of human flap endonuclease 1 to PCNA. *EMBO J* **24**: 683–693. https://doi.org/10.1038/sj.emboj.7600519

Sebesta M, Cooper CDO, Ariza A, Carnie CJ, Ahel D (2017) Structural insights into the function of ZRANB3 in replication stress response. *Nat Commun* **8**: 15847. https://doi.org/10.1038/ncomms15847

Strzalka W, Oyama T, Tori K, Morikawa K (2009) Crystal structures of the *Arabidopsis thaliana* proliferating cell nuclear antigen 1 and 2 proteins complexed with the human p21 C-terminal segment. *Protein Sci* **18**: 1072–1080. https://doi.org/10.1002/pro.117

Tsutakawa SE, Classen S, Chapados BR, Arvai AS, Finger LD, Guenther G, Tomlinson CG, Thompson P, Sarker AH, Shen B, Cooper PK, Grasby JA, Tainer JA (2011) Human flap endonuclease structures, DNA double-base flipping, and a unified understanding of the FEN1 superfamily. *Cell* **145**: 198–211. https://doi.org/10.1016/j.cell.2011.03.004

Warbrick E (1998) PCNA binding through a conserved motif. *Bioessays* **20**: 195–199. https://doi.org/10.1002/(SICI)1521-1878(199803)20:3<195::AID-BIES2>3.0.CO;2-R

Yao NY, O'Donnell M (2012) The RFC clamp loader: structure and function. *Subcell Biochem* **62**: 259–279. https://doi.org/10.1007/978-94-007-4572-8_14